Title

Avidity-Based Method for the Efficient Generation of Monoubiquitinated Recombinant Proteins

Journal

Journal of the American Chemical Society, 145(14)

ISSN

0002-7863

Authors

Nelson, Spencer L
Li, Yunan
Chen, Yue
et al.

Publication Date

2023-04-12

DOI

10.1021/jacs.3c01943

Peer reviewed

JACS
JOURNAL OF THE AMERICAN CHEMICAL SOCIETY

pubs.acs.org/JACS

Communication

Avidity-Based Method for the Efficient Generation of Monoubiquitinated Recombinant Proteins

Spencer L. Nelson, Yunan Li, Yue Chen, and Lalit Deshmukh*

Cite This: J. Am. Chem. Soc. 2023, 145, 7748−7752

Read Online

ACCESS | Metrics & More | Article Recommendations | Supporting Information

ABSTRACT: Monoubiquitination of proteins governs diverse physiological processes, and its dysregulation is implicated in multiple pathologies. The difficulty of preparing sufficient material often complicates the biophysical studies of monoubiquitinated recombinant proteins. Here we describe a robust avidity-based method that overcomes this problem. As a proof-of-concept, we produced milligram quantities of two monoubiquitinated targets, Parkinson's protein α-synuclein and ESCRT-protein ALIX, using NEDD4-family E3 ligases. Monoubiquitination hotspots were identified by quantitative chemical proteomics. Using FRAP and dye-binding assays, we uncovered strikingly opposite effects of monoubiquitination on the phase separation and fibrillization properties of these two amyloidogenic proteins, reflecting differences in their intermolecular interactions, thereby providing unique insights into the impact of monoubiquitination on protein aggregation.

Protein ubiquitination orchestrates nearly all eukaryotic cellular events.[1] It starts by attaching ubiquitin through isopeptide bonds to a single or multiple lysine residues of a target protein via a coordinated enzymatic reaction involving activating (E1), conjugating (E2), and ligating (E3) enzymes to form mono/multi-monoubiquitinated products. Further modification of ubiquitin's seven lysine residues and its N-terminal methionine creates moieties decorated with poly-ubiquitin chains. These post-translational modifications (mono-, multimono-, and polyubiquitination) encode specific signals that are decoded by deubiquitinating enzymes and proteins containing ubiquitin-binding domains. Among these, monoubiquitination is the most prevalent,[2] and is involved in various physiological processes (e.g., chromatin regulation, DNA damage response, protein sorting, trafficking, and degradation), viral egress, genetic disorders, and neuro-degenerative proteinopathies.[3] Although the mechanisms that restrict the substrates to monoubiquitination, preventing polyubiquitination, are not clearly understood, monoubiquitinated proteins are often modified at multiple individual sites, creating a pool of heterogeneous populations.[4,5] The frequency with which each site gets ubiquitinated and the collective effects of these modifications on the physicochemical characteristics of the target protein are usually unclear since obtaining such samples in sufficiently high yields and purities for biophysical studies is challenging. This is because enzymatic reactions performed on recombinant substrates often generate a composite mixture containing reaction components and mono-, multimono-, and polyubiquitinated products, and selective purification of monoubiquitinated species from this soup is difficult. Additionally, chemical (nonenzymatic) methods that can produce isopeptide-linked monoubiquitinated proteins are technically challenging and not applicable to most proteins.[6] There is, therefore, a need for a technique that can facilitate the high-yield production of monoubiquitinated proteins. Here we present an efficient approach that fills this gap.

This method can be applied to recombinant substrates with specific ubiquitinating enzymes. As a proof-of-concept, we used two substrates, α-synuclein and apoptosis-linked gene-2-interacting protein X (ALIX), and enzymes UbE1, UbE2D3, and neuronal precursor cell-expressed developmentally down-regulated 4 (NEDD4)-family E3 ligases (NEDD4L and WW domain containing E3 ubiquitin protein ligase 2 (WWP2)); Figure 1A. Aberrant aggregation of α-synuclein is a hallmark of Parkinson's disease.[7,8] α-synuclein accumulated in the Lewy bodies of Parkinson's patients is often mono- and diubiquitinated,[9] perhaps due to the breakdown of its degradation pathways. Endosomal sorting complex required for transport (ESCRT)-protein ALIX governs multiple processes, including protein sorting, neurodevelopment, cytokinesis, and enveloped virus budding.[10−12] Like many ESCRT-proteins, ALIX undergoes monoubiquitination in vivo.[13,14] All nine members of the NEDD4-family ligases collaborate with UbE1 and UbE2D3 to promote the ubiquitination of cellular proteins.[8] Specifically, NEDD4L ubiquitinates α-synuclein in the postischemic brain, promoting its degradation via the endolysosomal pathway,[15] whereas NEDD4L and WWP2 are involved in ALIX's monoubiquitination, vital for its roles in human immunodeficiency virus 1 (HIV-1) budding[16] and lysosomal sorting of G protein coupled receptors (GPCRs).[17] Although mono- and polyubiquitinated α-synuclein was produced using chemical methods,[18−20] no such attempts were made for ALIX, due to

Received: February 21, 2023
Published: April 3, 2023

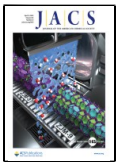

https://doi.org/10.1021/jacs.3c01943
J. Am. Chem. Soc. 2023, 145, 7748−7752

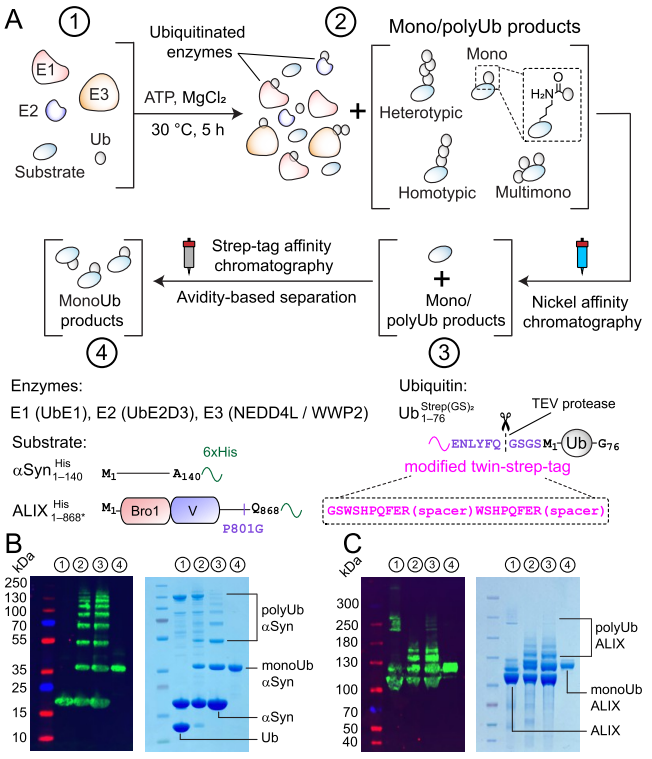

Figure 1. Large-scale production of monoubiquitinated proteins. (A) In vitro ubiquitination reaction (Step 1) to produce ubiquitinated products with native isopeptide linkages, highlighted in the dashed square (Step 2). The lower panel denotes the constructs that were used (Figure S1 and Table S1). The reaction components were subjected to affinity chromatography (Steps 3 and 4) for a selective purification of monoubiquitinated products. Western blot and SDS-PAGE analyses of corresponding reactions of (B) αSyn^{His}_{1-140} + NEDD4L and (C) $ALIX^{His}_{1-868*}$ + WWP2; 4−12% Bis-Tris and 3−8% Tris-Acetate gels were used for αSyn^{His}_{1-140} and $ALIX^{His}_{1-868*}$, respectively. Aliquots from each step are designated by a circled number.

the problems associated with its recombinant expression stemming from ribosomal stalling induced by its amyloidogenic proline-rich domain (PRD).[12,21] We recently overcame these expression issues by introducing a P801G mutation in its PRD and established that ALIX phase separates via its PRD, crucial for its role in cytokinetic abscission (manuscript submitted). However, the effects of monoubiquitination on ALIX's aggregation and functions are unclear.

All recombinant enzymes were expressed with N-terminal polyhistidine affinity tags, which were cleaved using tobacco etch virus (TEV)-protease during the final stages of purification. α-synuclein and ALIX were expressed with noncleavable C-terminal polyhistidine tags, αSyn^{His}_{1-140} and $ALIX^{His}_{1-868*}$ (the asterisk denotes P801G mutation), respectively; Figure 1A. The ubiquitin construct carried a modified N-terminal twin-strep tag[22] and a TEV-protease cleavage site, $Ub^{Strep(GS)_2}_{1-762}$; see Figure S1 for the rationale used for the design of this tag and Figures S2 and S3 for the nuclear magnetic resonance (NMR) analyses of $Ub^{Strep(GS)_2}_{1-762}$, which revealed a minimal impact of the tag on ubiquitin's structure. The enzymes and $Ub^{Strep(GS)_2}_{1-762}$ were mixed with substrates (αSyn^{His}_{1-140}/$ALIX^{His}_{1-868*}$) and incubated with ATP and $MgCl_2$ to generate mono-, multimono-, and polyubiquitinated products. Nickel affinity chromatography facilitated a selective purification of substrate and its ubiquitinated products. Monoubiquitinated species were separated from this mixture using strep-tag affinity chromatography by exploiting the avidity effect.[23] This is because unlike monoubiquitinated products, multimono-/polyubiquitinated moieties bound extremely tightly to the resin-coupled strep-tactin, a derivative of tetrameric streptavidin, and therefore, could not be readily displaced by the competitive binding reagent, biotin (Figures S4 and S5). Western blot and sodium dodecyl-sulfate polyacrylamide gel electrophoresis (SDS-PAGE) analyses of αSyn^{His}_{1-140} + NEDD4L and $ALIX^{His}_{1-868*}$ + WWP2 reactions and purification of monoubiquitinated products are shown in Figure 1B−C. Both reactions generated milligram quantities of monoubiquitinated products (Figures S6 and S7 and Table S2), attesting to the efficacy of this method.

The high purity of the monoubiquitinated α-synuclein facilitated a detailed stoichiometric analysis using our chemical proteomics approach (Figure 2A−C).[24] Here, unmodified lysine residues of a target protein are conjugated to an acetyl-GG-*N*-Hydroxysuccinimide (NHS) tag, followed by proteolytic digestion and secondary labeling with ^{13}C-acetyl-NHS, thereby generating fragments of the originally ubiquitinated peptides and their unmodified counterparts that are structurally identical but differ in ^{13}C-labeling (Figure 2B). Subsequent liquid chromatography-mass spectrometry (LC-MS) analysis of these fragments allows quantification of site-specific monoubiquitination frequency via a comparison of the corresponding chromatography peak-area ratios (Figure 2C and Table S3). The N-terminal membrane binding region (MBR), central nonamyloid component (NAC), and C-terminal region (CTR) of α-synuclein were monoubiquitinated by NEDD4L at 37%, 21%, and 42%, respectively. The collective high-frequency (63%) of monoubiquitination of residues in the NAC (K80) and CTR (K96/K97/K102) of α-synuclein is consistent with the fact that NEDD4-ligases bind to the proline-rich region of its CTR.[8,25] Although the stoichiometric deconvolution of immediately adjacent lysine residues (e.g., K96/K97/K102 of the CTR) was not feasible, we were able to quantify monoubiquitination frequencies for sufficiently distant residues of the MBR (e.g., 19% monoubiquitination at K6/K10/K12 vs 11% at K21/K23). A similar analysis of multimono/polyubiquitinated α-synuclein produced in these ubiquitination reactions revealed changes in enzymatic preferences upon progressive addition of ubiquitin moieties (Figure S4B and Table S4). Similar quantification of cerebral α-synuclein is difficult owing to endogenous deubiquitinating enzymes and the rapid deubiquitination in post-mortem samples.[25] Hence, the above approach identifies ubiquitination hotspots for a given group of enzymes and their substrate and provides important insights regarding the corresponding in vivo ubiquitination pattern for the said group.

Both unmodified and monoubiquitinated α-synuclein phase separated into condensates with a molecular crowder polyethylene glycol (PEG)-8000, Figures 2D and S8−S9. Although freshly made condensates of both moieties were dynamic, as evidenced by fluorescence recovery after photobleaching (FRAP) assays (Figure 2E), condensates of α-synuclein exhibited a noticeably lower fluorescence recovery than those of its monoubiquitinated counterpart (60% vs 80% average recovery in 150 s, respectively). Moreover, the fluorescence recovery of α-synuclein condensates decreased significantly after a 2 h incubation at room temperature, whereas the condensates of monoubiquitinated α-synuclein remained dynamic (20% vs 75% recovery, respectively). The latter

https://doi.org/10.1021/jacs.3c01943
J. Am. Chem. Soc. 2023, 145, 7748−7752

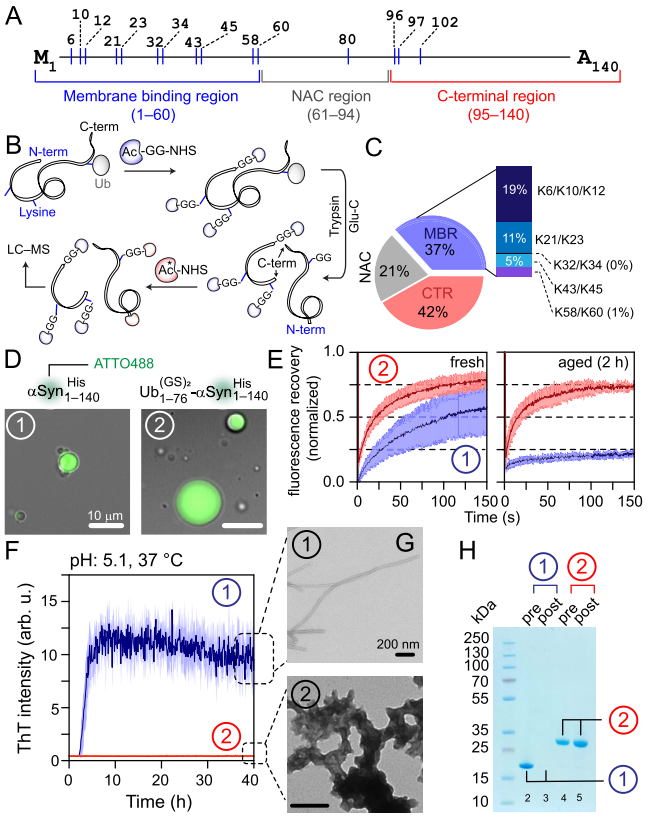

Figure 2. Impact of NEDD4L-mediated monoubiquitination on α-synuclein's aggregation. Schemes of (A) α-synuclein and (B) quantitative chemical proteomics used to determine monoubiquitination stoichiometry; the asterisk denotes ^{13}C-labeled acetyl-NHS. (C) Pie-chart of the average frequency of monoubiquitination in the MBR (blue), NAC (gray) and CTR (red) regions of αSyn^{His}_{1-140} (n = 2). Unlike the CTR, the monoubiquitination frequency for the individual lysine residues of MBR could be deconvoluted, represented by a stacked bar. (D) Microscopy images of droplets of αSyn^{His}_{1-140} and its monoubiquitinated counterpart with 10% w/v PEG-8000, represented by circled no. 1 and 2, respectively; the same numbering scheme is used in the remaining panels. (E) FRAP analysis of freshly prepared and aged condensates with the solid line and shaded region representing the mean and SD (n = 3), and blue and red colors for unmodified and monoubiquitinated αSyn^{His}_{1-140}, respectively. (F) Aggregation of non- and monoubiquitinated αSyn^{His}_{1-140} studied by ThT assays (n = 2); the same color-scheme as E. (G) Negative-stain EM images of aggregated samples from F showing fibrils for αSyn^{His}_{1-140} and amorphous aggregates for its monoubiquitinated moieties. (H) SDS-PAGE analysis of pre- and postaggregated samples from F. The lack of band intensity in lane-3 is due to αSyn^{His}_{1-140} fibrillization.

frequently coalesced and increased significantly in size with time (Video S1). These observations indicate a time-dependent gelation of α-synuclein droplets, perhaps due to its fibrillization and the lack thereof for its monoubiquitinated moieties. Aggregation assays performed using an amyloid-sensitive dye, Thioflavin T (ThT), confirmed this hypothesis, with sigmoidal aggregation profiles for α-synuclein, a hallmark of fibrillization, and no noticeable increase in ThT signals for its monoubiquitinated counterpart (Figure 2F). Negative-stain electron microscopy (EM) and SDS-PAGE analyses demonstrated the presence of SDS-resistant fibrils and nonfibrillar aggregates for unmodified and monoubiquitinated α-synuclein, respectively (Figure 2G–H). These results demonstrate that NEDD4L-mediated monoubiquitination of α-synuclein creates dynamic condensates and makes it resistant to fibrillization. This is likely due to modifications of lysine residues in and around its aggregation-prone NAC region,[26,27] thereby preventing fibrillization through modulation of intermolecular interactions.

Solution NMR analysis established that the ALIX-V domain binds to ubiquitin, Figures 3A–B and S10, consistent with a prior report that measured a dissociation constant of ~120 μM for this interaction.[28] Analysis of monoubiquitinated $ALIX^{His}_{1-868*}$ using quantitative chemical proteomics showed that the V-domain is significantly more monoubiquitinated by NEDD4L and WWP2 (72% and 60% monoubiquitination,

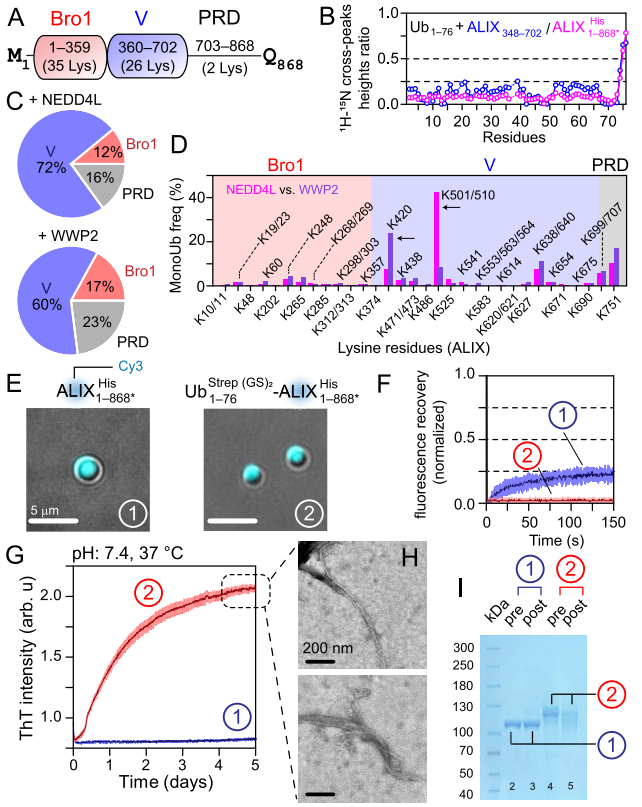

Figure 3. NEDD4L/WWP2-mediated monoubiquitination of ALIX. (A) Scheme of ALIX (also see Figure S11). (B) The reduction in $^1H_N/^{15}N$ cross-peak heights of 100 μM ^{15}N-labeled ubiquitin with 100 μM nonlabeled $ALIX_{348-702}$ (blue) and $ALIX^{His}_{1-868*}$ (pink). (C) Pie-charts illustrating the average frequency of monoubiquitination in individual ALIX domains using NEDD4L (upper) and WWP2 (lower); n = 2. (D) Bar-chart of site-specific differences in monoubiquitination frequencies of ALIX residues brought out by NEDD4L (pink) and WWP2 (magenta); arrows mark significant differences. Only ubiquitinated residues are plotted. (E) Microscopy images of condensates of $ALIX^{His}_{1-868*}$ and its WWP2-mediated monoubiquitinated counterpart (5% w/v PEG-4000), represented by circled no. 1 and 2; the same numbering scheme is used in the remaining panels. (F) Poor FRAP recoveries (<25%) for the freshly prepared condensates of $ALIX^{His}_{1-868*}$ (blue) and its WWP2-mediated monoubiquitinated moieties (red), n = 3, the same coloring scheme in the remaining panels. (G) Fibrillization of monoubiquitinated $ALIX^{His}_{1-868*}$ and the lack thereof for its nonubiquitinated species by ThT assays, n = 2. (H) Negative-stain EM analyses of fibrils formed by monoubiquitinated $ALIX^{His}_{1-868*}$. (I) SDS-PAGE analysis of pre- and postaggregated samples from G. Fibrillization of monoubiquitinated ALIX resulted in a decreased band intensity in lane-5 as compared to the preaggregated sample in lane-4.

https://doi.org/10.1021/jacs.3c01943
J. Am. Chem. Soc. 2023, 145, 7748–7752

respectively, Figure 3C and Table S3) than Bro1 and PRD of ALIX. Examination of site-specific frequencies revealed two significant differences (Figure 3D). Residues K501/K510 of V-domain were monoubiquitinated at 44% vs 9% while residue K420 was monoubiquitinated at 8% vs 24% by NEDD4L and WWP2, respectively, highlighting the site-specific preferences of these two ligases. ALIX and its monoubiquitinated counterpart formed gel-like condensates with PEG-4000, as evidenced by fluorescence microscopy and negligible FRAP recoveries (Figures 3E−F and S8 and S9), consistent with our recent findings that ALIX makes nondynamic condensates that confine abscission factors (manuscript submitted). Unlike α-synuclein (cf. Figure 2E), monoubiquitinated ALIX did not form dynamic condensates (Figure 3F and S12A), possibly because monoubiquitinated ALIX molecules bound to one another via their V-domains, thereby creating optimal conditions for nucleation and growth of ALIX fibrils. ThT assays, negative-stain EM, and SDS-PAGE analyses confirmed this hypothesis and revealed that, unlike unmodified ALIX, its monoubiquitinated counterpart formed amyloid fibrils (Figures 3G−I and S12B). Such fibrils in vivo will likely act as a scaffolding platform, aiding the formation of downstream ESCRT filaments needed for membrane scission, thereby facilitating ALIX's versatile functions.

In summary, we devised an efficient method to purify milligram quantities of monoubiquitinated proteins. It facilitated detailed analyses of ubiquitination hotspots and the impact of monoubiquitination on α-synuclein and ALIX aggregation. This study utilized recombinant NEDD4-E3 ligases, which ubiquitinate targets at multiple sites. Given its ease-of-use, this method will apply to similar systems, including ligases that modify a specific lysine, and lays a solid foundation for our ongoing efforts to produce polyubiquitinated recombinant proteins. Additionally, it will serve as a template to generate small ubiquitin-related modifier (SUMO)-ylated proteins,[29] a posttranslational modification analogous to ubiquitination.

■ ASSOCIATED CONTENT

Data Availability Statement

Human UbE1 (UniProt accession no. P22314), UbE2D3 (UniProt accession no. P61077), NEDD4L (UniProt accession no. Q96PU5), WWP2 (UniProt accession no. O00308), ubiquitin (UniProt accession no. P0CG48), α-synuclein (UniProt accession no. P37840), and ALIX (UniProt accession no. Q8WUM4). The constructs of $Ub^{Strep(GS)_2}_{1-762}$, UbE1, UbE2D3, NEDD4L, WWP2, $ALIX^{His}_{1-868*}$, $ALIX_{348-702}$, and αSyn^{His}_{1-140} have been deposited in the Addgene repository as accession numbers 186803, 186804, 186805, 186806, 186807, 186808, 189819, and 186802, respectively. The NMR chemical shift assignments of $Ub^{Strep(GS)_2}_{1-762}$ have been deposited in the Biological Magnetic Resonance Bank as entry 51647. The mass spectrometry proteomics data have been deposited to the ProteomeXchange Consortium via the PRIDE partner repository as entry PXD037416.

Supporting Information

The Supporting Information is available free of charge at https://pubs.acs.org/doi/10.1021/jacs.3c01943.

Experimental details, recombinant constructs used in current study, NMR chemical shift analysis of ubiquitin constructs used in current study, Backbone RDC analysis of $Ub^{Strep(GS)_2}_{1-76}$, exploiting the avidity effect for the selective purification of monoubiquitinated species, Strep-tag affinity chromatography for a selective purification of monoubiquitinated moieties, mass spectrometry analysis of monoubiquitinated α-synuclein and ALIX, solution NMR analysis of monoubiquitinated α-synuclein, phase separation of α-synuclein and ALIX and the impact of monoubiquitination, panoramic images showing the phase separation of proteins used in current study, NMR analyses of ubiquitin−ALIX interactions, ALIX and the location of its lysine residues, aggregation properties of NEDD4L-mediated monoubiquitinated ALIX, recombinant constructs used in current study, components of in vitro ubiquitination reactions and the yields of corresponding monoubiquitinated products, quantification of the site-specific frequency of monoubiquitination αSyn^{His}_{1-140} and $ALIX^{His}_{1-868*}$ using a chemical proteomics approach, and quantification of the site-specific frequency of multi-mono/polyubiquitinated αSyn^{His}_{1-140} using chemical proteomics approach (PDF)

Video S1: Droplet fusion of unmodified and monoubiquitinated α-synuclein (AVI)

■ AUTHOR INFORMATION

Corresponding Author

Lalit Deshmukh − *Department of Chemistry and Biochemistry, University of California San Diego, La Jolla, California 92093, United States;* orcid.org/0000-0001-6126-1560; Email: ldeshmukh@ucsd.edu

Authors

Spencer L. Nelson − *Department of Chemistry and Biochemistry, University of California San Diego, La Jolla, California 92093, United States;* orcid.org/0000-0003-4819-4441

Yunan Li − *Department of Biochemistry, Molecular Biology, and Biophysics, University of Minnesota at Twin Cities, Minneapolis, Minnesota 55455, United States*

Yue Chen − *Department of Biochemistry, Molecular Biology, and Biophysics, University of Minnesota at Twin Cities, Minneapolis, Minnesota 55455, United States;* orcid.org/0000-0002-0153-9927

Complete contact information is available at: https://pubs.acs.org/10.1021/jacs.3c01943

Notes

The authors declare no competing financial interest.

■ ACKNOWLEDGMENTS

The authors thank Z. Jiang, R. Ghirlando, C. McHugh, I. Budin, and P. A. Jennings for useful discussions and Y. Su, X. Huang, G. Castillon, and P. Guo for mass spectrometry, NMR, negative-stain EM, and fluorescence imaging support, respectively. This work was funded by the NIH Grant R35 GM147708 (to L.D.), NSF Grant CHE-1753154 (to Y.C.), and NIH Grant R35 GM124896 (to Y.C.).

■ REFERENCES

(1) Swatek, K. N.; Komander, D. Ubiquitin modifications. *Cell Res.* **2016**, *26* (4), 399−422.

(2) Kaiser, S. E.; Riley, B. E.; Shaler, T. A.; Trevino, R. S.; Becker, C. H.; Schulman, H.; Kopito, R. R. Protein standard absolute

quantification (PSAQ) method for the measurement of cellular ubiquitin pools. *Nat. Methods* **2011**, *8* (8), 691−696.
(3) Chen, Y.; Zhou, D.; Yao, Y.; Sun, Y.; Yao, F.; Ma, L. Monoubiquitination in homeostasis and cancer. *Int. J. Mol. Sci.* **2022**, *23* (11), 5925.
(4) Rott, R.; Szargel, R.; Haskin, J.; Shani, V.; Shainskaya, A.; Manov, I.; Liani, E.; Avraham, E.; Engelender, S. Monoubiquitylation of alpha-synuclein by seven in absentia homolog (SIAH) promotes its aggregation in dopaminergic cells. *J. Biol. Chem.* **2008**, *283* (6), 3316−3328.
(5) Nakagawa, T.; Nakayama, K. Protein monoubiquitylation: targets and diverse functions. *Genes Cells* **2015**, *20* (7), 543−62.
(6) Stanley, M.; Virdee, S. Chemical ubiquitination for decrypting a cellular code. *Biochem. J.* **2016**, *473* (10), 1297−314.
(7) Stefanis, L. α-Synuclein in Parkinson's disease. *Cold Spring Harb. Perspect. Med.* **2012**, *2* (2), a009399.
(8) Conway, J. A.; Kinsman, G.; Kramer, E. R. The role of NEDD4 E3 ubiquitin−protein ligases in Parkinson's disease. *Genes* **2022**, *13* (3), 513.
(9) Tofaris, G. K.; Razzaq, A.; Ghetti, B.; Lilley, K. S.; Spillantini, M. G. Ubiquitination of α-synuclein in Lewy bodies is a pathological event not associated with impairment of proteasome function. *J. Biol. Chem.* **2003**, *278* (45), 44405−11.
(10) Odorizzi, G. The multiple personalities of ALIX. *J. Cell Sci.* **2006**, *119* (15), 3025−3032.
(11) Laporte, M. H.; Chatellard, C.; Vauchez, V.; Hemming, F. J.; Deloulme, J.-C.; Vossier, F.; Blot, B.; Fraboulet, S.; Sadoul, R. ALIX is required during development for normal growth of the mouse brain. *Sci. Rep.* **2017**, *7* (1), 44767.
(12) Elias, R. D.; Ma, W.; Ghirlando, R.; Schwieters, C. D.; Reddy, V. S.; Deshmukh, L. Proline-rich domain of human ALIX contains multiple TSG101-UEV interaction sites and forms phosphorylation-mediated reversible amyloids. *Proc. Natl. Acad. Sci. U.S.A.* **2020**, *117* (39), 24274−24284.
(13) Sette, P.; Jadwin, J. A.; Dussupt, V.; Bello, N. F.; Bouamr, F. The ESCRT-associated protein ALIX recruits the ubiquitin ligase NEDD4−1 to facilitate HIV-1 release through the LYPXnL L domain motif. *J. Virol.* **2010**, *84* (16), 8181−92.
(14) Korbei, B. Ubiquitination of the ubiquitin-binding machinery: how early ESCRT components are controlled. *Essays Biochem.* **2022**, *66* (2), 169−177.
(15) Kim, T.; Chokkalla, A. K.; Vemuganti, R. Deletion of ubiquitin ligase NEDD4L exacerbates ischemic brain damage. *J. Cereb. Blood Flow Metab.* **2021**, *41* (5), 1058−1066.
(16) Votteler, J.; Sundquist, W. I. Virus budding and the ESCRT pathway. *Cell Host Microbe* **2013**, *14* (3), 232−41.
(17) Dores, M. R.; Lin, H.; Grimsey, N. J.; Mendez, F.; Trejo, J. The α-arrestin ARRDC3 mediates ALIX ubiquitination and G protein−coupled receptor lysosomal sorting. *Mol. Biol. Cell* **2015**, *26* (25), 4660−4673.
(18) Hejjaoui, M.; Haj-Yahya, M.; Kumar, K. S. A.; Brik, A.; Lashuel, H. A. Towards elucidation of the role of ubiquitination in the pathogenesis of Parkinson's disease with semisynthetic ubiquitinated α-synuclein. *Angew. Chem., Int. Ed. Engl.* **2011**, *50* (2), 405−409.
(19) Haj-Yahya, M.; Fauvet, B.; Herman-Bachinsky, Y.; Hejjaoui, M.; Bavikar, S. N.; Karthikeyan, S. V.; Ciechanover, A.; Lashuel, H. A.; Brik, A. Synthetic polyubiquitinated α-Synuclein reveals important insights into the roles of the ubiquitin chain in regulating its pathophysiology. *Proc. Natl. Acad. Sci. U.S.A.* **2013**, *110* (44), 17726−17731.
(20) Meier, F.; Abeywardana, T.; Dhall, A.; Marotta, N. P.; Varkey, J.; Langen, R.; Chatterjee, C.; Pratt, M. R. Semisynthetic, site-specific ubiquitin modification of α-synuclein reveals differential effects on aggregation. *J. Am. Chem. Soc.* **2012**, *134* (12), 5468−5471.
(21) Elias, R. D.; Ramaraju, B.; Deshmukh, L. Mechanistic roles of tyrosine phosphorylation in reversible amyloids, autoinhibition, and endosomal membrane association of ALIX. *J. Biol. Chem.* **2021**, *297* (5), 101328.
(22) Schmidt, T. G. M.; Batz, L.; Bonet, L.; Carl, U.; Holzapfel, G.; Kiem, K.; Matulewicz, K.; Niermeier, D.; Schuchardt, I.; Stanar, K. Development of the Twin-Strep-tag and its application for purification of recombinant proteins from cell culture supernatants. *Protein Expr. Purif.* **2013**, *92* (1), 54−61.
(23) Erlendsson, S.; Teilum, K. Binding revisited—avidity in cellular function and signaling. *Front. Mol. Biosci.* **2021**, DOI: 10.3389/fmolb.2020.615565.
(24) Li, Y.; Evers, J.; Luo, A.; Erber, L.; Postler, Z.; Chen, Y. A quantitative chemical proteomics approach for site-specific stoichiometry analysis of ubiquitination. *Angew. Chem., Int. Ed. Engl.* **2019**, *58* (2), 537−541.
(25) Tofaris, G. K.; Kim, H. T.; Hourez, R.; Jung, J. W.; Kim, K. P.; Goldberg, A. L. Ubiquitin ligase NEDD4 promotes α-synuclein degradation by the endosomal-lysosomal pathway. *Proc. Natl. Acad. Sci. U.S.A.* **2011**, *108* (41), 17004−9.
(26) Rodriguez, J. A.; Ivanova, M. I.; Sawaya, M. R.; Cascio, D.; Reyes, F. E.; Shi, D.; Sangwan, S.; Guenther, E. L.; Johnson, L. M.; Zhang, M.; Jiang, L.; Arbing, M. A.; Nannenga, B. L.; Hattne, J.; Whitelegge, J.; Brewster, A. S.; Messerschmidt, M.; Boutet, S.; Sauter, N. K.; Gonen, T.; Eisenberg, D. S. Structure of the toxic core of α-synuclein from invisible crystals. *Nature* **2015**, *525* (7570), 486−90.
(27) Guerrero-Ferreira, R.; Taylor, N. M. I.; Mona, D.; Ringler, P.; Lauer, M. E.; Riek, R.; Britschgi, M.; Stahlberg, H. Cryo-EM structure of α-synuclein fibrils. *eLife* **2018**, *7*, e36402.
(28) Keren-Kaplan, T.; Attali, I.; Estrin, M.; Kuo, L. S.; Farkash, E.; Jerabek-Willemsen, M.; Blutraich, N.; Artzi, S.; Peri, A.; Freed, E. O.; Wolfson, H. J.; Prag, G. Structure-based in silico identification of ubiquitin-binding domains provides insights into the ALIX-V:ubiquitin complex and retrovirus budding. *EMBO J.* **2013**, *32* (4), 538−551.
(29) Geiss-Friedlander, R.; Melchior, F. Concepts in sumoylation: a decade on. *Nat. Rev. Mol. Cell Biol.* **2007**, *8* (12), 947−956.

https://doi.org/10.1021/jacs.3c01943
J. Am. Chem. Soc. 2023, 145, 7748−7752